10.1016/0038-1101(93)90237-K

Solid-State Electronics Vol. 36, No. 5, pp. 697–703, 1993
Printed in Great Britain.

0038-1101/93 $6.00 + 0.00

ACOUSTO-ELECTRIC DEEP-LEVEL TRANSIENT SPECTROSCOPY IN SEMICONDUCTORS

A. ABBATE†, K. J. HAN, I. V. OSTROVSKII‡ and P. DAS

Electrical, Computer and Systems Engineering Department, Rensselaer Polytechnic Institute, Troy, NY 12180-3950, U.S.A.

(Received 3 October 1992; in revised form 18 November 1992)

Abstract—The electric field, generated by the propagation of a surface acoustic wave on a piezoelectric crystal, is used as a probing tool to study the transient behavior of deep levels. This field interacts with the free carriers present in the semiconductor resulting in an alteration of the carrier density at the surface of the semiconductor. The rate at which these excess charges are induced at the semiconductor surface, or diminished after the passage of the SAW pulse, can be related to the position and the cross section of the deep levels in the semiconductor. The technique is employed to study deep levels in a GaAs epilayer grown on semi-insulating GaAs substrate. The theoretical analysis of the transient phenomenon is presented along with experimental verification. Due to the analogy to DLTS measurements we refer to this technique as acousto-electric deep-level transient spectroscopy (AEDLTS).

1. INTRODUCTION

Acoustic-electric (ae) measurement on semiconductors can be used to study deep trap levels. The nonlinear acousto-electric interaction between the surface acoustic wave (SAW) electric field and the free carriers in a semiconductor has been extensively studied[1–3]. As a result of this interaction, a voltage, commonly called the transverse acousto-electric voltage (TAV), is generated across the semiconductor. Two possible testing structures can be used in TAV experiments, these are the combined-medium and separate-medium structures. In the conbined-medium structure, the SAW is generated directly on a piezoelectric semiconductor such as GaAs and CdS; by converse action the propagating elastic wave induces in the semiconductor the radiofrequency (rf) electric field. If the semiconductor is not piezoelectric, such as Si, the SAW is generated on a piezoelectric crystal such as $LiNbO_3$ and the semiconductor is placed on top of the free surface[4]. Even in this case the acoustic wave induces an rf electric field which decays exponentially into the semiconductor. This is the separate-medium structure. In this case the analysis of TAV transients is more complex[5], but the calculations presented in this paper are still valid.

The combined-medium structure used to generate the surface acoustic wave (SAW) and the TAV, in the experiments presented in this paper is shown in Fig. 1. The SAW is generated by applying a rf electrical voltage across the input interdigital transducer (IDT). Once generated, the acoustic wave propagates on the semiconductor surface. The semiconductor sample consists of a (100) n-type GaAs epitaxial layer (epilayer), 8 μm thick, grown by MOCVD process on top of a semi-insulating (SI) GaAs substrate. The electron concentration in the epilayer was measured to be $1.3 \times 10^{14}\,cm^{-3}$[6]. The metal contact on top of the epilayer is used to create a Schottky diode and thus to deplete of free carriers the region below. The energy of the acoustic wave in the semiconductor is mainly restricted into a region with depth about the SAW wavelength ($\simeq 40\,\mu$m in our case), therefore probing is mainly restricted to the epilayer and to part of the substrate. It has to be pointed out that the testing structure is also used as a signal processing device, namely the acoustic charge transport (ACT) device[7].

TAV measurements have been used to characterize a large variety of semiconductor properties, among those: interface states' density[8,9], junction depth [10], mobility[11] and deep trap levels ionization energy[12]. In practical cases, the surface acoustic wave is modulated as a sequence of pulses with a repetition period of seconds. The resulting TAV signal resembles a square wave with rise and fall times sometimes in the range of μs even though the time constants associated with the SAW pulse are in the ns range (Fig. 2). Transient measurements of the acousto-electric voltage generated in semiconductors have also been used in the past[8]. Generally, it has been observed that the decay constant of the TAV signal is more sensitive to external perturbations such as incident light source and temperature, than the overall TAV amplitude.

The importance of trapping effects in acousto-electric phenomena has been recognized and described in various papers[1,3,13]. At the end of the rf pulse, there remains a transverse voltage due to

†Permanent address: Benet Labs, Watervliet, NY 12189–4050, U.S.A.
‡Permanent address: Kiev State University, Prospekt Pobeda, 73/1, k.38 Kiev 252062, Ukraine.

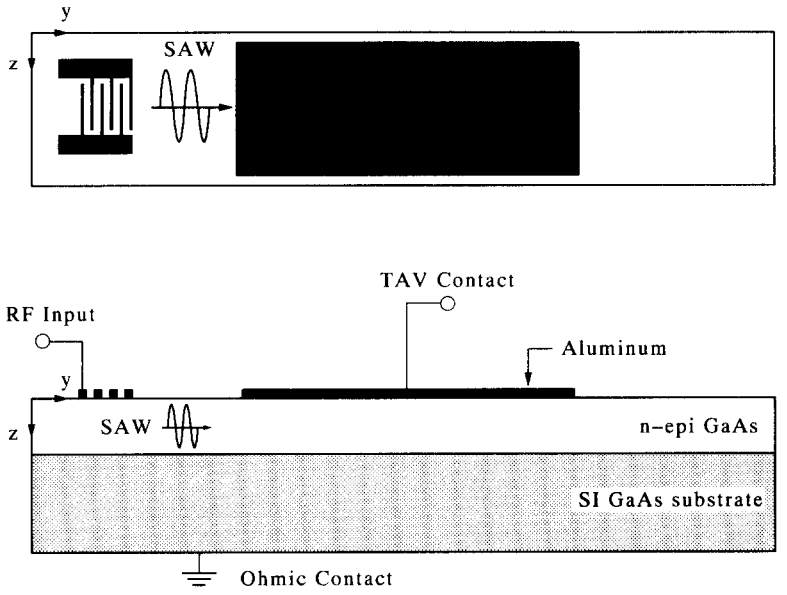

Fig. 1. Semiconductor structure used for experiments. An n-type epilayer ($n = 1.3 \times 10^{14}$ cm^{-3}) was grown on SI GaAs. The SAW is generated by applying a voltage to the RF input and the TAV is detected by the large metal contact.

charged (or discharged) traps, and this voltage decays to zero as the system returns to its initial equilibrium. This component of the TAV, due to the trapped charge, often has the same sign of the acousto-electric part; but it has been observed that in some published experimental meaurements the two components can have different sign[13]. An analytical expression for the change in trap occupancy and its effects on the TAV signal is presented along with some experimental verification.

The TAV fall time can be used to detect and study trap levels in the semiconductor; the trap energy and cross section can be easily measured by monitoring the change in τ_F as a function of the sample temperature or of the energy of an incident light beam.

2. THEORETICAL ANALYSIS OF THE TAV TRANSIENT RESPONSE

Using the Shockley and Read theory[14], the steady-state density of trap levels filled with electrons, n_{t_0}, can be calculated as

$$n_{t_0} = \frac{C_n n_0 + C_p p_1}{C_n(n_0 + n_1) + C_p(p_0 + p_1)} N_t \tag{1}$$

$$p_{t_0} = N_t - n_{t_0} \tag{2}$$

where the terms have the well-known definitions[15]. It is common use in literature to define the trap level lifetime τ; for reasons of simplicity, we have chosen to use the quantity $\omega_t = \tau^{-1}$, referred as the trap angular frequency and defined as follows

$$\omega_t = C_n(n_0 + n_1) + C_p(p_0 + p_1). \tag{3}$$

Once the rf electric field of the SAW is applied, the generation and recombination rates differ from their equilibrium values. Using a small signal approach, the rf variation of the trapped charge (v) is calculated as follows

$$v = \frac{C_n p_{t_0} n' - C_p n_{t_0} p'}{j\omega + \omega_t + C_n n' + C_p p'} \tag{4}$$

where n' and p' are the small signal perturbations of the carrier concentrations, and $\omega = 2\pi f_{SAW}$ is the SAW angular frequency. The terms n' and p' are calculated by solving the semiconductor's constitutive equations. From boundary conditions at the surface of the material, it can be shown that these terms are proportional to the square root of the SAW power[2].

The small signal recombination rates are defined by the following relations

$$r_n = C_n p_{t_0} n' - C_n(n_0 + n_1)v - C_n n' v \tag{5}$$

$$r_p = C_p n_{t_0} p' + C_p(p_0 + p_1)v + C_p p' v. \tag{6}$$

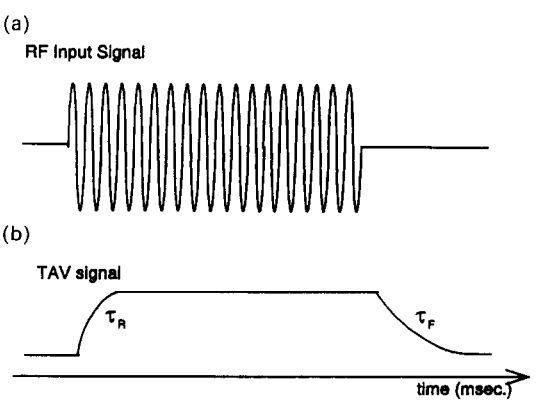

Fig. 2. Time signals of the rf input used to generate the SAW (a) and of the resulting TAV signal (b).

Equations (5) and (6) must be averaged over the SAW period. The net average for the first two terms in the right-hand sides are null, while the last terms in both equations have a non-zero contribution. These two terms, $C_n \cdot n' \cdot v$ and $C_p \cdot p' \cdot v$, are the nonlinear terms of generation and recombination and are added to the d.c. continuity equations

$$\langle r_n \rangle = -G_n^{(nl)} = -C_n \cdot \langle n' \cdot v^* \rangle \quad (7)$$

$$\langle r_p \rangle = -G_p^{(nl)} = +C_p \cdot \langle p' \cdot v^* \rangle. \quad (8)$$

The inherent nonlinearity of the recombination–generation processes produces a net change in the trapped charge, an effect which is analogous to the nonlinear current which generates the TAV. As the SAW pulse is switched off, the excess trapped charge will be re-emitted and the TAV voltage will return to zero with the characteristic time associated with the trap level.

In the approximation of an extrinsic semiconductor in which the majority carrier concentration is not perturbed by the SAW, we can write

$$R_n = C_n N_t n_0 - C_n(n_0 + n_1)(n_{t_0} + \Delta n_{t_0}) - G_n^{(nl)} \quad (9)$$

$$R_p = C_p(p_0 + p_1)(n_{t_0} + \Delta n_{t_0}) - C_p N_t p_1 - G_p^{(nl)} \quad (10)$$

where Δn_{t_0} represents the variation in trap occupancy due to the acousto-electric field.

The system being in steady-state, we must impose

$$R_n - R_p = \frac{\partial n_t}{\partial t} = \frac{\partial(n_{t_0} + \Delta n_{t_0})}{\partial t} \doteq 0 \quad (11)$$

and thus we obtain, for the variation in trap occupancy, the following

$$\Delta n_{t_0}^{(dc)} = \frac{G_n^{(nl)} - G_p^{(nl)}}{C_n(n_0 + n_1) + C_p(p_0 + p_1)} = \frac{G_n^{(nl)} - G_p^{(nl)}}{\omega_t}. \quad (12)$$

The term $\Delta n_{t_0}^{(dc)}$ represents the change in occupancy of the trap level due to the acousto-electric interaction and in particular to the nonlinearity of the generation–recombination processes at the trap level. Trapping effects due to the acousto-electric interaction in the TAV fall time can be observed even in the case in which the semiconductor is extrinsic and the SAW power is not high enough to perturb the majority carrier concentration.

At the end of the SAW pulse, the acousto-electric component of the TAV decays to zero almost instantaneously (the time constant is given by the sample relaxation time), while a voltage component due to the trapped charge remains and decays to zero with a characteristic time τ_F (Fig. 2).

The trapped charge is expressed as

$$\Delta n_t(t) = \Delta n_{t_0} \cdot e^{-t/\tau_F} \quad (13)$$

with

$$\tau_F^{-1} = \omega_t = C_n(n_0 + n_1) + C_p(p_0 + p_1). \quad (14)$$

The TAV signal measured on the oscilloscope (Fig. 2) can be expressed as follows

$$\mathrm{TAV}(t) = \mathrm{TAV}_0 \cdot e^{-t/\tau_F}. \quad (15)$$

This analysis was obtained assuming only one trap level, since the acousto-electric interaction does mainly affect the occupancy of the trap level close in energy to the Fermi level. However, the result can be readily generalized.

3. EFFECTS OF DEEP-LEVELS ON THE TAV AMPLITUDE

The SAW propagating on a piezoelectric medium generates an electric field at the same frequency of the stress wave. From the expression of this electric field[3,16], the nonlinear acousto-electric current in the semiconductor is calculated as

$$\langle J_{nl} \rangle = \tfrac{1}{2} \mathrm{Re}[\sigma_{ae}(y) \cdot E_{ae}^*(y)] \quad (16)$$

and the total steady-state d.c. electric field is calculated using the Poisson, continuity and current equations in the d.c. domain[17]. The integration of this electric field across the semiconductor yields the TAV. An analytical expression for the TAV amplitude is

$$\mathrm{TAV} = P_{SAW} \cdot K_{ae} \cdot K_t \quad (17)$$

where P_{SAW} is the SAW power per unit length, K_{ae} depends on the conductivity of the sample and is practically independent of P_{SAW}; K_t represents the attenuation term due to recombination and generation and thus is function of the trap occupancy.

The various terms can be expressed as follows[18]

$$K_{ae} = V_0 \cdot \frac{n\mu_n - p\mu_p}{n\mu_n + p\mu_p} \cdot \frac{1}{(\gamma^2 + 1)^2 + 4\omega^2 R^2} \quad (18)$$

where

$$R = \frac{\omega_{cn}\omega_{dn}^2 + \omega_{cp}\omega_{dp}^2}{(\omega_{cn}\omega_{dn} + \omega_{cp}\omega_{dp})^2} \cdot \gamma \quad (19)$$

and ω_{cn} and ω_{cp} are the dielectric relaxation frequency for electron and holes, respectively; ω_{dn} and ω_{dp} are the diffusion frequency for electron and holes, respectively, and γ is calculated from the characteristic equation of the system and given by

$$\gamma = \sqrt{1 + \frac{\omega_{cn}\omega_{dn} + \omega_{cp}\omega_{dp}}{\omega^2}}. \quad (20)$$

The term V_0 is a constant and a function of various material's parameters[18].

The term K_t represents the attenuation of the TAV amplitude due to the presence of traps, and is given by

$$K_t = \frac{1 + \omega^2 R^2}{(1 + R_t)^2 + \omega^2 R^2} \quad (21)$$

where

$$R_t = \frac{V_{SAW}}{\omega}\left(\frac{C_n}{D_n} p_t + \frac{C_p}{D_p} n_t\right). \quad (22)$$

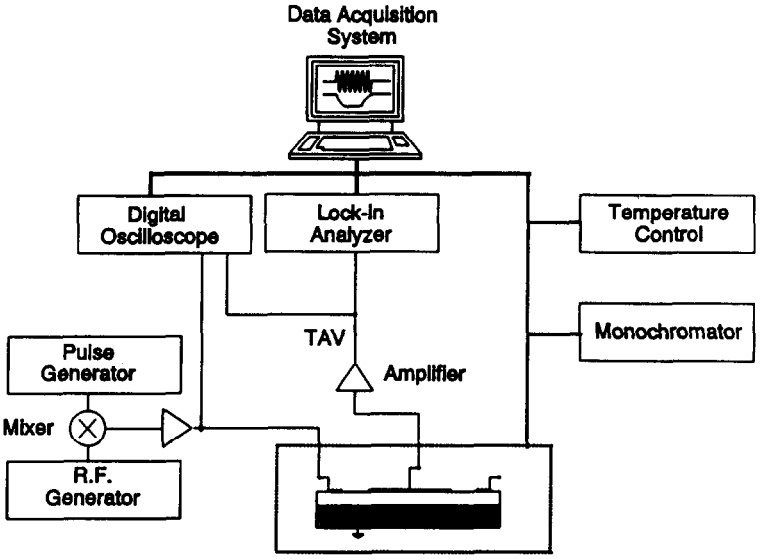

Fig. 3. Experimental setup used for AEDLTS measurements.

From eqns (21)–(22) we can easily see that as the term R_t increases, K_t does decrease and thus also the TAV. If there are no trap levels, the term K_t is equal to one.

4. EXPERIMENTAL VERIFICATION

The experimental apparatus shown in Fig. 3 was used. The TAV output signal is picked up through the Schottky metal contact and a high input impedance amplifier is used to minimize external circuitry loading effects. Time plots of a typical RF input signal (trace A) and of the output TAV signal (trace B) are shown in Fig. 2. The TAV rise and fall time constants τ_R and τ_F, can be of the order of ms even though the time associated with the input RF signal are of the order of 10 ns.

From the theory presented, the change in occupancy of the trap is a function of the SAW power. In Fig. 4, the TAV is plotted as a fuction of the SAW power. The asterisk defines the experimentally measured values of TAV, while the continuous line expresses the theoretical value of the TAV amplitude, assuming K_t constant [eqn (17)]. The experimental values of TAV are well below the theoretical line since as the SAW power is increased, a change in the trap occupancy occurs resulting in a decrease of K_t.

In Fig. 5, the ratio between the measured TAV and the applied SAW power (P_{SAW}) is plotted as a function of P_{SAW}. In the range of values of applied SAW power, the term K_{ae} can be considered constant; this assumption was verified by a measurement of the change in d.c. conductivity of the epilayer as function of the SAW power[19]. Therefore the decrease in the ratio TAV/P_{SAW} as function of the SAW power is to be related to the change in K_t and thus in the change in trap occupancy. Another evidence of the validity of our approach is given by the measurement shown in Fig. 6. Different TAV vs applied bias

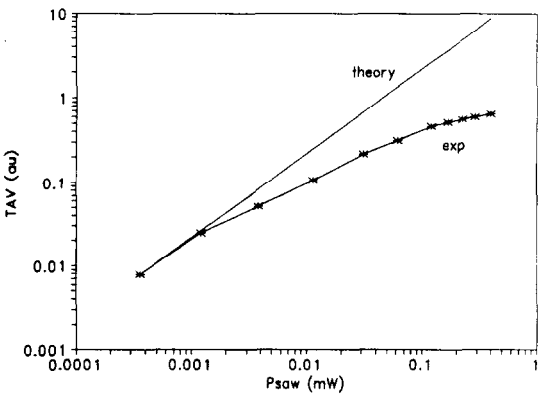

Fig. 4. Plot of the TAV amplitude as a function of the SAW power. The asterisks refer to the experimental values while the continuous line represents the theoretically expected values neglecting the effect of charge trapping.

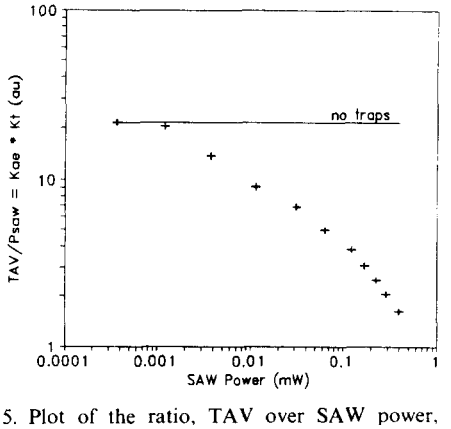

Fig. 5. Plot of the ratio, TAV over SAW power, as a function of the SAW power. The symbols represent the experimental values. Neglecting the presence of traps we would expect the ratio to be constant, as shown by the straight line.

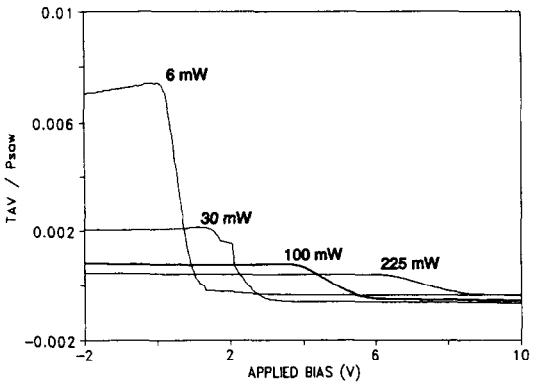

Fig. 6. Plot of the ratio, TAV over SAW power, as a function of applied bias. The different value of SAW power for each curve is expressed as a parameter.

voltage are plotted with the SAW power as a parameter. In this figure the TAV amplitude is normalized by the SAW power. The d.c. bias voltage is applied on the Schottky contact in order to deplete the region beneath it; the value of bias votage, for which the TAV amplitude is zero, V_b, can be used to evaluate the amount of surface-state charge at the metal-semiconductor contact, and thus is related to the barrier height of the metal–semiconductor junction. With increasing SAW power, the TAV curves are shifted to the right, even though the TAV/P_{SAW} ratio does decrease. Any change in the ratio TAV/P_{SAW} is due to changes in K_t and thus the shift toward higher biases of the zero crossing voltage is to be attributed to a change in occupancy of the trap levels[20,21]. From the theory of the Schottky barrier we can express the change in V_b as follows

$$q \cdot \Delta V_b \sim \Delta\phi_B = -\Delta\phi_0 = \frac{KT}{n_t} \cdot \Delta n_t \qquad (23)$$

where q is the electron charge and ϕ_0 represents the energy level below which all trap states are filled and above which they can be considered empty. For an n-type extrinsic semiconductor, assuming $C_n \gg C_p$, the change in occupancy of the level can be expressed as

$$\Delta n_t^{(dc)} \simeq A \frac{C_n}{2\omega_t} p_t (P_{SAW})^{1/2} \qquad (24)$$

where the constant A is calculated numerically by solving the system of equations described in Section 3. It has to be mentioned that the constant A in eqn (27) is not necessarily positive, its sign depends on the conditions existing in the semiconductor. For example in the case that the interaction region is depleted of free electrons, the constant A is negative. From eqns (23) and (24) it is clear that the shift in V_b is proportional to the square root of the SAW power. This relation is expressed in Fig. 7, where the experimental values of V_b are plotted together with the values calculated using eqn (27). The agreement is very good, and it confirms the validity of our theory. The zero SAW power value of V_b is zero, because it represents only the contribution to the barrier height of the trapped charge at the contact. For low SAW power the influence of trapped charge on the barrier height is reduced and the values obtained are close to those of an ideal Schottky barrier.

5. TAV TRANSIENT MEASUREMENTS ON GaAs

The measured TAV fall time is mainly sensitive to the trap level near the Fermi level (E_f), thus if the Fermi level is varied by other means, such as temperature, bias voltage or light, the TAV transient can be used to characterize the trap levels[22]. Measurements of TAV transients as a function of temperature were already discussed in various papers[7]. Such measurements are similar to the conventional DLTS technique[22], their usefulness laying in the characterization of high resistivity materials, since DLTS is limited to semiconductors with free-carrier concentrations larger than the deep trap level concentrations[23]. Also it has been suggested to utilize TAV measurements in conjunction with illumination to perform DLTS[24]. As shown in Fig. 8(B), the SAW is generated and as the acousto-electric interaction reaches steady-state, a light pulse is shone on the sample. As a result a variation of the TAV amplitude is observed, and the transient is recorded. Since the TAV is a function of the surface conductivity of the sample, this experiment is equivalent to surface photovoltage or photoconductivity transient measurements[25]. From the transient measurement, the thermal cross sections are obtained.

A different kind of experiment, in which the sample is illuminated by a monochromatic light is now presented. The effect of illumination is to photoionize deep levels so that they will be able to participate in the acousto-electric effect and thus in the emission process by which they are characterized. For this case, various signals are plotted in Fig. 8(A) as a function of time. By varying the wavelength of the

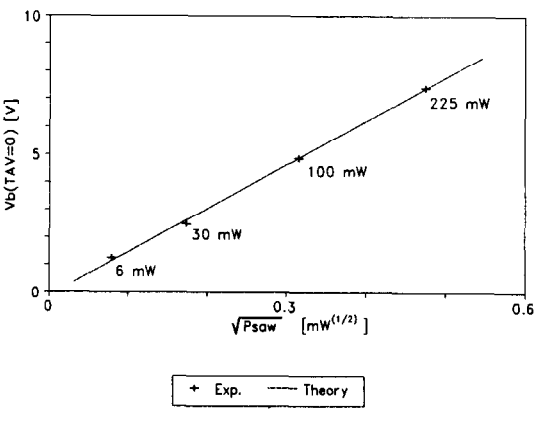

Fig. 7. Plot of the applied bias voltage V_b for which the measured TAV amplitude is zero. This voltage is proportional to the barrier height. The symbols represent the experimental values and the dashed line represents the theoretical value obtained from eqn (23).

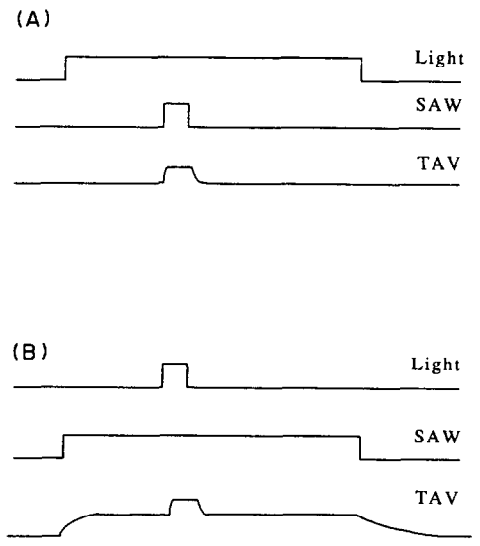

Fig. 8. Experimental time signals involved in optical AEDLTS measurements. (A) Time signals in the measurement proposed and used to measure the spectral distribution of the optical cross section of the EL2 level. (B) Time signals used in the complementary measurement presented in Ref. [24].

light, the ionization energies for different trap levels are detected, in addition to their corresponding optical cross sections. This method is analogous to the one presented by Gupta *et al.* in Ref. [27], where DLTS is performed by using a small voltage pulse in conjunction with steady-state illumination[26].

A Bausch and Lomb monochromator was used to illuminate the sample with incident photon energy varying from 0.5 to 1.3 eV. For each measurement, the semiconductor sample was in steady-state condition before, during and after the SAW pulse. Fig. 9 shows the digitized transient for the TAV in the dark and under a 0.848 eV illumination. The sharp change in the decay constant τ_F can be explained by considering the combined effects of illumination and acousto-electric interaction in the semiconductor. In the case of illumination, as shown in Fig. 8(A), the transient fall time is expressed by the following relationship

$$\tau_{F_L}^{-1} = [C_n(n_0 + n_1) + C_p(p_0 + p_1)] + \Phi\sigma^{(0)} = \tau_{F_D}^{-1} + \Phi\sigma^{(0)} \quad (25)$$

where τ_{F_L} and τ_{F_D} represent the measured TAV fall times under steady state illumination and in the dark, respectively; Φ is the light intensity and $\sigma^{(0)}$ is the optical cross section. By measuring both time constants (τ_{F_L} and τ_{F_D}), eqn (28) yields the values of optical cross section. Results are shown in Fig. 10 as empty squares. The two lines represent measurements presented in literature for the EL2 room-temperature hole optical cross section[27,28]. There is some disagreement for the values of cross section measured for higher photon energies, at this time it was not possible to understand the reasons.

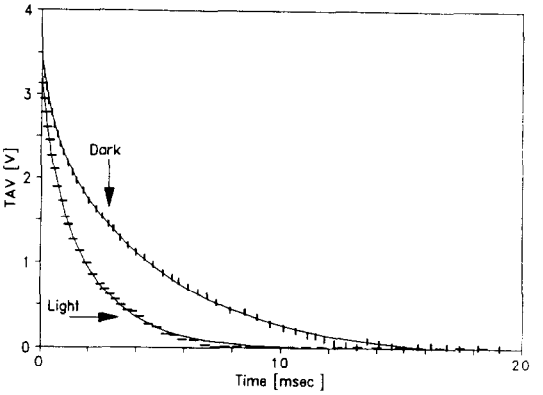

Fig. 9. TAV transient measurements performed in dark conditions and under illumination with a 0.848 eV monochrome light. The horizontal and vertical short dashes represent the experimental values, and the continuous lines represent the computer fits, calculated assuming a sum of exponential decays.

The thermal cross section σ_n for the trap level was also calculated from the measurement performed in the dark; the value obtained is 7.22×10^{-14} cm^2. This result agrees well with values obtained by other researchers for the EL2 level[29]. This result was also confirmed by temperature dependent TAV transient measurements[23].

6. CONCLUSIONS

Acousto-electric deep level transient spectroscopy (AEDLTS) can be used with a large variety of external excitations to study deep trap levels in semiconductors. The theorectical analysis of the TAV transient was included, along with experimental verification. The technique was utilized to study deep levels in a GaAs epilayer grown on semi-insulating GaAs substrate. Optical AEDLTS can be used to detect deep trap levels in semiconductor structures. In the example presented, the thermal cross section of the EL2 level in GaAs was measured, as well as the spectral distribution of its optical cross section.

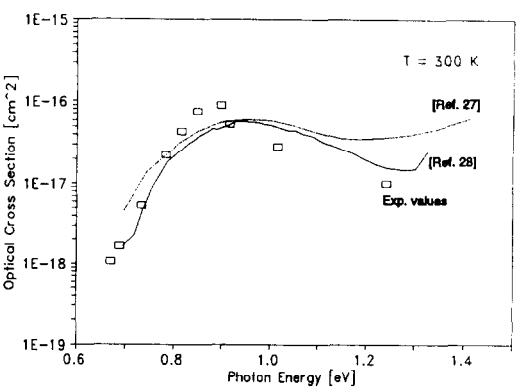

Fig. 10. Calculated values for the optical cross section of the EL2 level ($\sigma^{(0)}$) as a function of the incident photon energy. Lines refer to values obtained from Refs [27,28].

As proposed measurement is analogous to conventional DLTS measurements, all the improvements and discussions presented over the years on the DLTS technique are equally applicable for AEDLTS experiments. The measurements show the possibility of using TAV measurements on high resistivity semiconductors, leading to its utilization for characterizing deep levels in the midgap range. This is not possible using conventional DLTS, even tough high resistivity materials can be examined by optical excitation during DLTS in a technique commonly termed photo-induced transient spectroscopy (PITS).

Acknowledgement—The authors would like to thank F. Palma for helpful discussions.

REFERENCES

1. J. Fritz, *J. appl. Phys.* **52,** 6749 (1981).
2. F. Palma, *J. appl. Phys.* **66,** 292 (1989).
3. F. Palma, G. de Cesare, A. Abbate and P. Das, *IEEE Trans. Ultras., Ferroel. and Freq. Control* **UFFC-38,** 503 (1991).
4. J. H. McFee, *Physical Acoustic*, Vol 4A. Academic Press, New York (1966).
5. A. Stagni, G. de Cesare and F. Palma, *Solid-St. Electron.* **33,** 1005 (1990).
6. A. Abbate, K. J. Han and P. Das, to be published.
7. M. J. Hoskins and B. J. Hunsinger, *J. appl. Phys.* **52,** 413 (1984).
8. M. Tabib-Azar, Nam-Chun Park and P. Das, *Solid-St. Electron.* **30,** 705 (1987).
9. A. Abbate, P. Das, F. Palma and G. de Cesare, *Proc. IEEE Ultrasonics Symp.*, pp. 459–463 (1990).
10. B. Davari and P. Das, *Proc. IEEE Ultrasonic Symp.*, pp. 479 (1982).
11. A. Bers, J. H. Cafarella and B. E. Burke, *Appl. Phys. Lett.* **22,** 399 (1973).
12. K. J. Han, A. Abbate, I. B. Bhat and P. Das, *Appl. Phys. Lett.* **60,** 862 (1992).
13. Y. V. Gulayev, A. M. Kmita, A. V. Medved', V. P. Plesskii, N. N. Shibanova and V. N. Fedorets, *Sov. Phys. Solid St.* **17,** 2289 (1976).
14. W. Shockley and W. T. Read, *Phys. Rev.* **87,** 835 (1952).
15. A. Chiabrera, *Solid-St. Electron.* **15,** 277 (1972).
16. K. A. Ingebrigtsen, *J. appl. Phys.* **40,** 2681 (1969).
17. H. Gilboa and P. Das, *Nondestructive Evaluation of Electrical Properties of Semiconductors Using SAW*, ONR Tech. Rep. (1977).
18. M. Tabib-Azar, M. N. Abedin, A. Abbate and P. Das, *J. Vac. Sci. Technol.* **B9,** 95 (1991).
19. K. J. Han, PhD thesis, Rensselaer Polytechnic Institute (1992).
20. S. M. Sze, *Physics of Semiconductor Devices*, pp. 270–279 (1981).
21. R. S. Withers, *IEEE Trans. Sonics and Ultrasonics* **SU-31,** 117 (1984).
22. D. V. Lang, *J. appl. Phys.* **45,** 3023 (1974).
23. A. Chantre, G. Vincent and B. Bois, *Phys. Rev. B* **23,** 5335 (1981).
24. H. Estrada-Vazquez, PhD thesis, Rensselaer Polytechnic Institute (1983).
25. R. H. Bube, *Photoconductivity of Solids*. Wiley, New York (1960).
26. D. S. Gupta, M. M. Chandra and V. Kumar, *Physics status solidi* (a) **80,** K209 (1983).
27. A. Chantre, G. Vincent and D. Bois, *Phys. Rev. B* **23,** 5335 (1981).
28. P. Silverberg, P. Omling and L. Samuelson, *Appl. Phys. Lett.* **52,** 1689 (1988).
29. G. M. Martin, A. Miltonneau and A. Mircea, *Electron. Lett.* **13,** 191 (1977).